

SCATTERING FUNCTIONS FROM THE NAVAL COMMUNICATION CHANNELS DATASET

Jeffery C. Allen, Michael Reuter, Richard C. North

SPAWAR System Center, San Diego, CA

ABSTRACT

Representative scattering functions are presented from the Naval Communication Channels (NCC) Dataset. The NCC Dataset contains over-the-air measurements of a mobile HMMWV and a mobile Navy ship transmitting to a fixed shore site at 1 Mbps in the 225-400 MHz military UHF band. These HMMWV and ship experiments are representative of urban Marine Corps and the Naval littoral UHF line-of-sight (LOS) communication environments. For the ship operating off the coast, a single path model is appropriate with slow fading (1 Hz). For the ship in the harbor, a few large structures “punctuate” the scattering function with additional spreading to 30 μ s. In contrast, the HMMWV exhibited faster fading (10 Hz) and multiple paths spread to 7 μ s. The same “large-structure” effect is present with a few paths spread to 20 μ s.

1. BACKGROUND

The design of reliable communications requires that modulation and demodulation techniques compensate for the deleterious effects of the communication channel. Thus, one of the most important steps in the design of a reliable communication system is a characterization of the communication channel. Soundings of a military UHF LOS channel were collected at San Diego, California during January and February of 1998. Detailed descriptions of the equipment, experiments, algorithms, channel movies, and the NCC Datasets are available to researchers on the website [1]. Channel estimation based on adaptive filter techniques, which included a demodulation scheme robust to multipath fading, performed exceptionally well in all scenarios. In contrast, conventional baseband channel estimation techniques, which require a separate and blind demodulator, were sometimes stymied by multipath. This paper presents selected channels for the ship and HMMWV estimated by the adaptive filter technique.

2. EQUIPMENT

Figure 1 shows the configuration of the mobile transmitter and the fixed-site receiver. A 511 pseudorandom

bit pattern was continuously transmitted from the mobile using BPSK at 231.5 MHz, 40 Watts, 999,995 bps on a raised cosine waveform. Over-the-air operation in the San Diego area requires an OA/9123 multicoupler as a pre- and post-selection filter to prevent the Tx jamming of nearby receivers and to reduce adjacent channel effects when Rx signal strength is low. The signal was sampled using the AST195 at 12 Msps to obtain approximately 5.6 seconds of contiguous data. The SABRE GPS beacon system transmitted once a minute on UHF LOS at 270.75 MHz. The received GPS beacon information was displayed on a JMCIS terminal giving the location, bearing, velocity, and past track information.

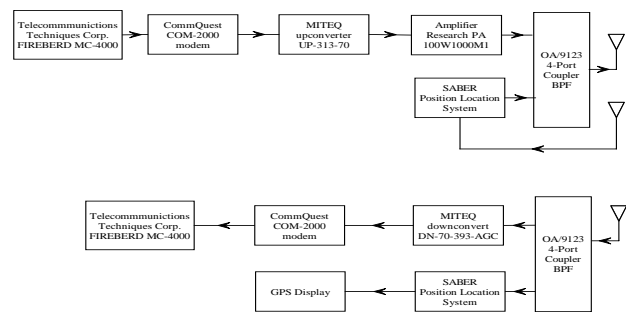


Figure 1: Tx and Rx configuration.

3. CHANNEL FUNCTIONS & ESTIMATORS

Bello’s seminal 1963 paper established the nomenclature and analysis for stochastic time-variant linear channels [2]. The *Input Delay-Spread function* $h(t, \tau)$ maps a transmitted signal $s(t)$ through a channel to the received signal $e(t)$ as [2, Eq. 9]:

$$e(t) = \int_{-\infty}^{\infty} h(t, t - \tau) s(\tau) d\tau. \quad (1)$$

Fourier transforming $h(t, \tau)$ in time gives the *Delay-Doppler-Spread function* [2, Eq. 28]:

$$U(f, \tau) = \int_{-\infty}^{\infty} e^{-j2\pi f t} h(t, \tau) dt. \quad (2)$$

With each channel function, Bello associates the corresponding covariance. For example, the covariance of $U(f, \tau)$ under WSSUS assumptions takes the form:

$$\begin{aligned} R_{UU}(f, \tau; f', \tau') &= E[U(f, \tau) \overline{U(f', \tau')}] \\ &= P(f, \tau) \delta(f - f') \delta(\tau - \tau'), \end{aligned} \quad (3)$$

where $P(f, \tau) = E[|U(f, \tau)|^2]$ is called the *scattering function*. The following examples show how these covariance functions encode the Doppler and delay distribution.

Example 3.1 (PMFS) *The Phase-Modulation Fading Simulator models a channel as [4]:*

$$h(t, \tau) = \frac{1}{\sqrt{N}} \sum_{n=1}^N a_n e^{+j2\pi f_n t} \delta(\tau - \tau_n). \quad (4)$$

Then the output $e(t)$ is a sum of delayed and frequency shifted versions of the transmitted signal:

$$e(t) = \frac{1}{\sqrt{N}} \sum_{n=1}^N a_n e^{+j2\pi f_n t} s(t - \tau_n). \quad (5)$$

The Delay-Doppler function $U(f, \tau)$ shows this “spread” in frequency and delay:

$$U(f, \tau) = \frac{1}{\sqrt{N}} \sum_{n=1}^N a_n \delta(f - f_n) \delta(\tau - \tau_n). \quad (6)$$

If the (a_n, f_n, τ_n) ’s are IID random variables with a_n ’s zero mean and independent from (f_n, τ_n) then $U(f, \tau)$ is a generalized random field with covariance [1, Eq. 2.3]:

$$R_{UU}(f, \tau; f', \tau') = \sigma_a^2 p_{f, \tau}(f, \tau) \delta(f - f') \delta(\tau - \tau'), \quad (7)$$

Thus, the scattering function registers the probability distribution $p_{f, \tau}(f, \tau)$ of the Doppler and delays.

Example 3.2 (QMFS) *Channels are also modeled with the Quadrature-Modulation Fading Simulator North & Zeidler [5], Crohn & Bonek [3], Proakis & Salehi [6, pages 697–703]:*

$$h(t, \tau) = \sum_{n=1}^N a_n(t) \delta(\tau - \tau_n). \quad (8)$$

Typically, the $\{a_n(t)\}$ ’s are complex-valued, JWSS uncorrelated Gaussian random processes with spectrum $P_{a_n a_n}(f)$ determined by the propagation environment. If the τ_n ’s are independent from the $\{a_n(t)\}$ ’s then

$$\begin{aligned} R_{UU}(f, \tau; f', \tau') &= \delta(f - f') \delta(\tau - \tau') \\ &\times \sum_{n=1}^N P_{a_n a_n}(f) p_{\tau_n}(\tau). \end{aligned} \quad (9)$$

Thus, the scattering function registers the delay and fading spectrum for each path.

These examples show that one must have a theoretical model to interpret the scattering function. In practice, the scattering function must be estimated from a finite number of discrete samples of the noisy, distorted, received signal demodulated to baseband. Consequently, these effects may confound interpretations of the scattering function. In our setup, the digital baseband Delay-Spread function $h_B(m, k)$ is smeared in delay by the raised cosine filter $x_{RC}(t)$ as [1, Section 3.4]:

$$h_B(m, k) = x_{RC} *_{\tau} h(mT/O_s, kT/O_s), \quad (10)$$

where $O_s=12$ is the oversampling rate. Then the digital baseband Delay-Doppler function $U_B(f, k)$ links to $U(f, \tau)$ as [1, Section 3.5]:

$$U_B(f, k) = x_{RC} *_{\tau} U(f, kT/O_s) \quad (11)$$

and the digital baseband scattering function $P_B(f, k)$ links to the scattering function $P(f, \tau)$ as

$$P_B(f, k) = x_{RC}^2 *_{\tau} P(f, kT/O_s). \quad (12)$$

Thus, the channel functions are smeared by the raised cosine filter.

Channel estimates are also corrupted by system distortion, noise, and demodulation effects. For this reason, the NCC Dataset also contains extensive files for calibration and emulated RF channels [1, Chapters 7 & 8]. Among candidate channel estimators, an adaptive filter estimate $h_{AF}(t, \tau)$ of $h(t, \tau)$ was found to be most robust against these effects. It has a spurious-free dynamic range of -42 dB and registers the distortion of the raised cosine caused by the OA/9123 multicoupler. A DFT of $h_{AF}(t, \tau)$ gives an estimate of the Delay-Doppler function. The estimated scattering function is obtained by averaging the magnitude square of these Delay-Doppler estimates.

As a final result, QMFS channel parameters are extracted and tabulated for subsequent use in RF channel

emulators. Specifically, best N -path channel models of the form

$$\tilde{h}(t, \tau) = \sum_{n=1}^N \tilde{a}_n(t) \delta(\tau - \tilde{\tau}_n) \quad (13)$$

are obtained as follows. For each $t_m = mT/O_s$, the 2-norm distance between $h_{AF}(m, :)$ and $\tilde{x}_{RC} *_{\tau} \tilde{h}(t_m, :)$ is minimized subject to physical and RF constraints. For example, the direct and reflected paths in the bluewater ship experiments cannot be resolved in time. Thus, only one path should be present. As the sum of two passive paths, its amplitude should be not exceed 2. More importantly, the multicoupler distorts the raised cosine. Attempts to fit a raised cosine model to this distorted data produce bogus paths. To correct for this distortion, a model for the distorted raised cosine $\tilde{x}_{RC}(t)$ was obtained from the laboratory reference data [1, Chapters 7 & 8]. This distorted raised cosine $\tilde{x}_{RC}(t)$ model is used to fit the channel.

4. SHIP: BLUEWATER

Data sets were collected from the USS Princeton (CG59) while departing San Diego Bay on 21 January, 1998 and off the coast of Point Loma on 22 January, 1998. These data sets are representative of the Naval littoral environment for the Military UHF band at ranges of 3 to 40 miles. Figure 2 is representative of the bluewater scattering function estimates. The trailing bands in delay arise from the raised-cosine waveform distorted by the OA/9123 multicoupler. To see this, Figure 3 shows the estimated PDP plotted against a reference PDP derived from the laboratory reference data. The standard two-path reflection model predicts a path delay of 0.44 ns. Combined with the sampling interval of 83 ns, the two paths have near-perfect overlap. Thus, the trailing bands arise from the distorted raised cosine waveform. With near perfect overlap, a single path model was fit to $h_{AF}(t, \tau)$ with the amplitude constraint $|\tilde{a}_1(t)| \leq 2$. The estimated fade rate $\tilde{f}_e \approx 0.54$ Hertz is in concordance with the maximal Doppler $f_D \approx 2.7$ Hertz. However, this amplitude estimate exhibits a slowly-varying trend that lowers the fade rate estimate and confounds PDF identification. When this trend was removed, the $\tilde{f}_e \approx 1$ Hertz and the detrended amplitude is identified as Gaussian or nominally Ricean with $K = (s/\sigma)^2 = 377$.

5. SHIP: HARBOR

In contrast to this bluewater data, Figure 4 shows the estimated scattering function for the ship in the San Diego harbor near the Coronado bridge. There is a

distinct second path delayed by $\Delta\tau \approx 2\mu\text{s}$ and shifted $\Delta f \approx -5$ Hertz from the direct path. In addition, multiple paths extending to 38 μs are present and these are also shifted by -5 Hertz. Figure 5 registers these delays in the estimated PDP and exhibits the strong second path. A 2-path fit to $h_{AF}(t, \tau)$ is also shown in Figure 5. These two paths are relatively uncorrelated and model most of the channel features. Table 1 reports the relevant path parameters as mean values referenced to Path 1 (f_e excepted).

Table 1: 2-Path fit to Harbor; Path 1 nominally Ricean; Correlation is 0.27.

Path	$\Delta\tau$	dB	Δf	f_e	PDF
1	0.0	0.0	0	1.6	Ricean: $K=136$
2	2.0	-4.9	-5	3.8	Ricean: $K=14.3$

6. HMMWV: URBAN FREEWAY

Representative of the HMMWV measurements is a channel sounding collected on January 16, 1998 at 13:25 while the HMMWV was driving south on I-5 near the San Diego airport at approximately 55 mph. Figure 6 plots the estimated power delay profile. The main lobe is wider than that of the laboratory or ship data and registers a secondary path at 18 μs relative delay implying that this channel is dispersive with respect to the 1 MHz bandwidth. Figure 7 plots the estimated scattering function and shows the secondary path is shifted by 13 Hertz. Moreover, there are several paths trailing the main path. Comparison with the power delay profile and the delay-spread function shows that these paths contribute to the extra width of the main lobe. In contrast to the simple two-path model for the ship, a multiple-path model is required to capture the features of this channel. A 4-path model was fit to the data. Paths 1, 2, and 3 track the main lobe while Path 4 tracks the secondary path. Figure 6 shows that this model fits the channel well. Table 2 records the results. Because Path 2 is slightly stronger than Path 1, the channel is non-minimum phase. Path 4 is relatively weaker and could be omitted from simulations. Also, the corresponding correlation matrix in Eq. 14 demonstrates that the mainlobe paths are highly correlated.

$$|\rho_{aa}| = \begin{bmatrix} 1.00 & 0.93 & 0.71 & 0.01 \\ 0.93 & 1.00 & 0.89 & 0.02 \\ 0.71 & 0.89 & 1.00 & 0.04 \\ 0.01 & 0.02 & 0.04 & 1.00 \end{bmatrix}. \quad (14)$$

Table 2: 4-Path fit to the HMMWV; Path 2 nominally Ricean.

Path	$\Delta\tau$	dB	Δf	f_e	PDF
1	0.00	0.0	0	7	Ricean: $K=2.6$
2	0.98	+0.5	0	7	Ricean: $K=1.1$
3	2.17	-4.1	1	6	Weibull: $K=2.0$
4	18.16	-20.5	13	4	Ricean: $K=19$

7. CONCLUSIONS

A methodology was presented to estimate and model communication channels of interest to the US Navy. For ship-to-shore bluewater operations, the channel sounding experiments demonstrate that the military band UHF LOS channel can be characterized using a flat fading model with a strong specular component. Thus, relatively high-data rates are possible for these operations using simple receiver architectures. In contrast, for littoral and HMMWV urban operations, large scale structures can induce strong multipath components that must be addressed with more complicated receiver structures coupled with lower data rates.

8. REFERENCES

- [1] Allen, J. C., M. Reuter, R. C. North [1998] *RF Channel Characterization & Estimation: Sequence-Based Methods Phase I*
<http://bobcat.spawar.navy.mil/hdrlos>.
- [2] Bello, Philip A. [1963] Characterization of Randomly Time-Variant Linear Channels, *IEEE Transactions on Communications Systems*, Vol. CS-11, pages 360–393.
- [3] Crohn, Ilan & Ernst Bonek [1992] Modeling of Intersymbol-Interference in a Rayleigh Fast Fading Channel with Typical Delay Power Profiles, *IEEE Transactions on Vehicular Technology*, Volume 41, Number 4, pages 438–446.
- [4] Hoeher, Peter [1992] A Statistical Discrete-Time Model for the WSSUS Multipath Channel, *IEEE Transactions on Vehicular Technology*, Vol 41, Number 4, pages 461–468.
- [5] North, Richard C. & James R. Zeidler [1994] Multi-channel Adaptive Equalization for Improved Performance in LOS Digital Radio, *1994 IEEE Military Communications Conference*, Fort Monmouth, NJ.
- [6] Proakis, John G. & Masoud Salehi [1994] *Communication Systems Engineering*, Prentice Hall, New Jersey.

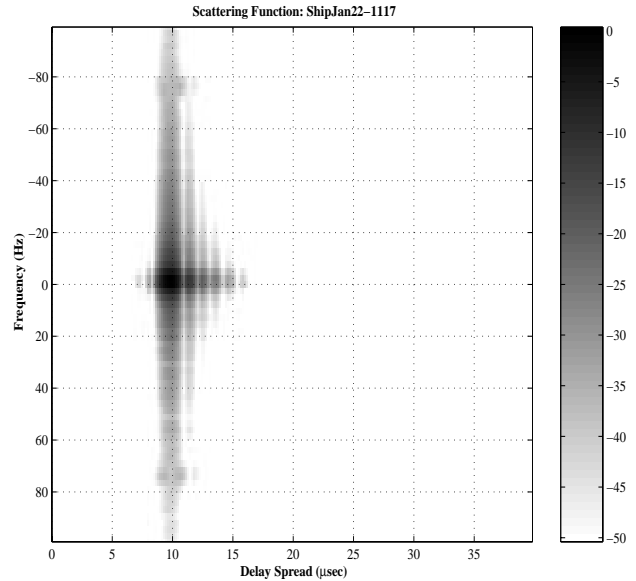


Figure 2: Bluewater scattering estimate 26.8 nm west of Point Loma; 14 averages.

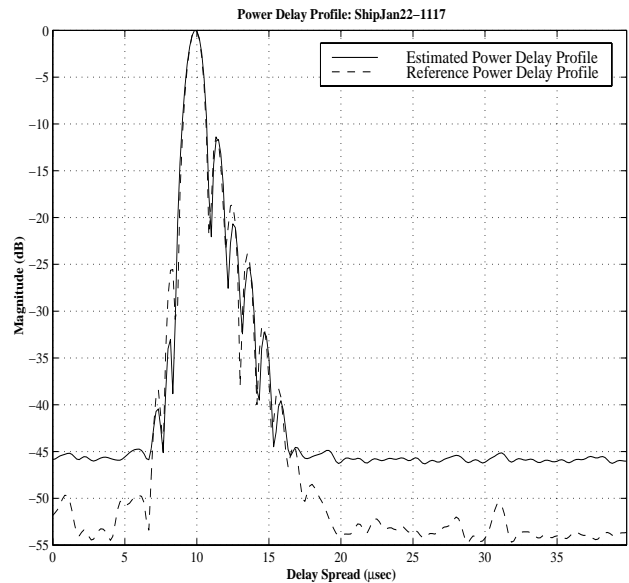


Figure 3: Bluewater power delay profile.

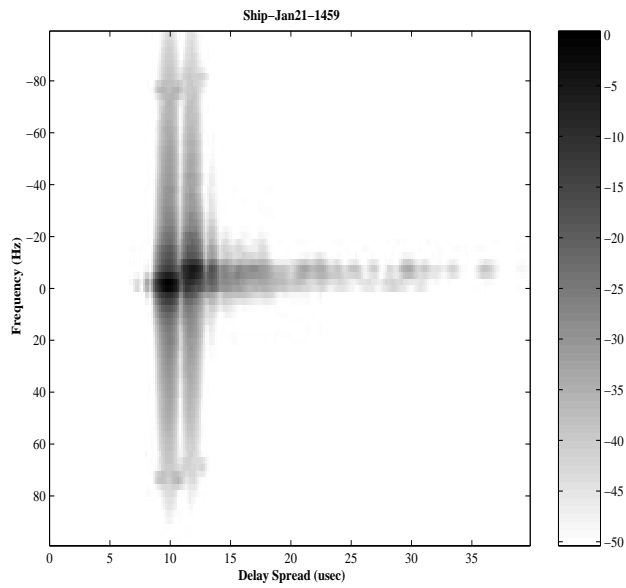


Figure 4: In harbor scattering estimate near Coronado Bridge; 14 averages.

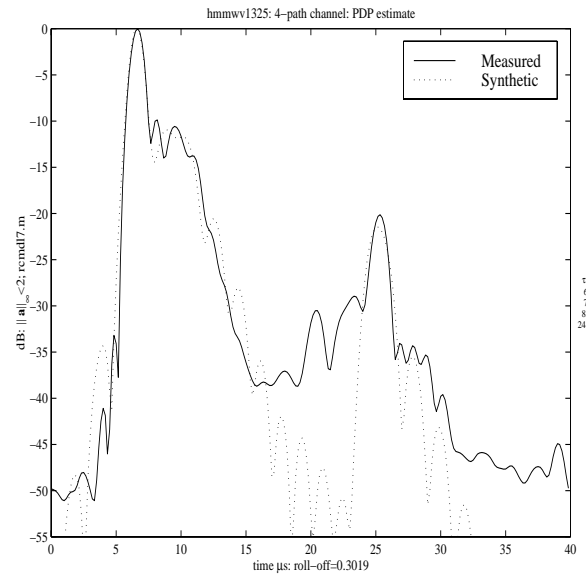


Figure 6: Power delay profile estimate for the HMMWV in San Diego (55 mph) and 4-path model.

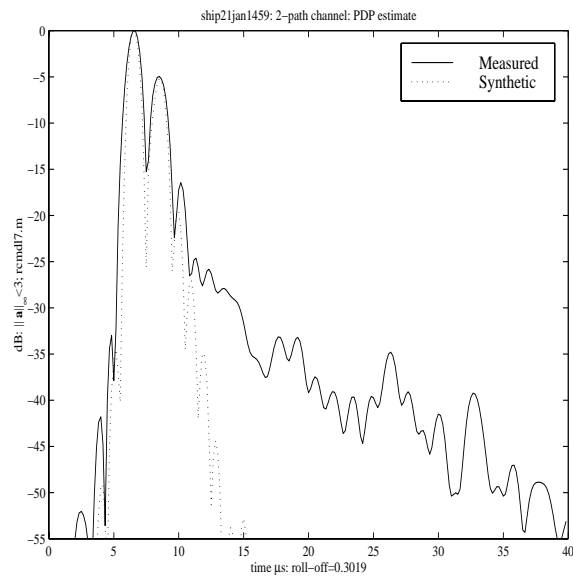


Figure 5: In harbor power delay profile and 2-path model.

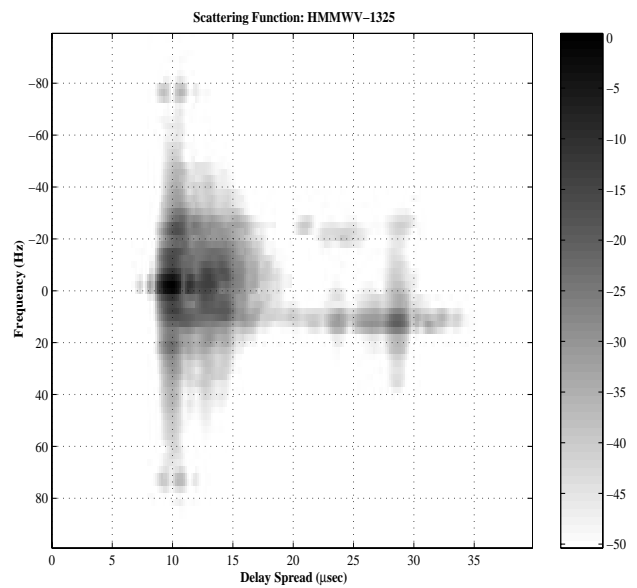


Figure 7: Scattering estimate for HMMWV in San Diego; 55 mph; 14 averages.